Reactions between atomic chlorine and pyridine in solid para-hydrogen: Infrared spectrum of the 1-chloropyridinyl (C5H5NCl) radical

Prasanta Das, Mohammed Bahou, and Yuan-Pern Lee

Citation: The Journal of Chemical Physics **138**, 054307 (2013); doi: 10.1063/1.4789407
View online: http://dx.doi.org/10.1063/1.4789407
View Table of Contents: http://scitation.aip.org/content/aip/journal/jcp/138/5?ver=pdfcov
Published by the AIP Publishing

Reactions between atomic chlorine and pyridine in solid *para*-hydrogen: Infrared spectrum of the 1-chloropyridinyl (C_5H_5N−Cl) radical

Prasanta Das,[1] Mohammed Bahou,[1] and Yuan-Pern Lee[1,2,a)]
[1]*Department of Applied Chemistry and Institute of Molecular Science, National Chiao Tung University, Hsinchu 30010, Taiwan*
[2]*Institute of Atomic and Molecular Sciences, Academia Sinica, Taipei 10617, Taiwan*

(Received 17 December 2012; accepted 10 January 2013; published online 6 February 2013)

With infrared absorption spectra we investigated the reaction between Cl atom and pyridine (C_5H_5N) in a *para*-hydrogen (p-H_2) matrix. Pyridine and Cl_2 were co-deposited with p-H_2 at 3.2 K; a planar C_5H_5N−Cl_2 complex was identified from the observed infrared spectrum of the Cl_2/C_5H_5N/p-H_2 matrix. Upon irradiation at 365 nm to generate Cl atom *in situ* and annealing at 5.1 K for 3 min to induce secondary reaction, the 1-chloropyridinyl radical (C_5H_5N−Cl) was identified as the major product of the reaction Cl + C_5H_5N in solid p-H_2; absorption lines at 3075.9, 1449.7, 1200.6, 1148.8, 1069.3, 1017.4, 742.9, and 688.7 cm^{-1} were observed. The assignments are based on comparison of observed vibrational wavenumbers and relative IR intensities with those predicted using the B3PW91/6-311++G(2d, 2p) method. The observation of the preferential addition of Cl to the N-site of pyridine to form C_5H_5N−Cl radical but not 2-, 3-, or 4-chloropyridine (ClC_5H_5N) radicals is consistent with the reported theoretical prediction that formation of the former proceeds via a barrierless path. © *2013 American Institute of Physics*. [http://dx.doi.org/10.1063/1.4789407]

I. INTRODUCTION

The reaction of atomic chlorine (Cl) with pyridine (C_5H_5N) has drawn much attention in atmospheric chemistry because pyridine is emitted into the atmosphere as a result of industrial activities such as the production of insecticides and herbicides and the combustion of coal; Cl atoms might have concentrations large enough to oxidize atmospheric pollutants in the marine and coastal atmosphere.[1–3] This reaction is important also in organic chemistry because the selectivity of tertiary versus primary hydrogen abstraction in photochlorination reactions is enhanced significantly when the reactions are conducted in solvents such as benzene and pyridine; the selectivity is attributed to formation of weakly bound complexes between Cl and benzene or pyridine.[4–9] The use of pyridine ester templates to direct selective steroid chlorination has also been investigated; the results indicate that the Cl atom coordinates to the N atom in pyridine before being relayed to a geometrically accessible substrate hydrogen.[10] From a fundamental point of view, the sites of pyridine selectively attacked by Cl and the nature of the bonding, whether σ- or π-bonding, between Cl atom and pyridine have important implications.[11–13]

Breslow *et al.* irradiated a solution of Cl_2 and C_5H_5N in CCl_4 with light at 355 nm and observed an absorption feature with λ_{max} = 334 nm;[11] they assigned this feature to charge-transfer band of 1-chloropyridinyl radical (C_5H_5N–Cl). They also performed calculations with the INDO/S (intermediate neglect of differential overlap) ROHF-CI (configuration interaction with restricted open-shell Hartree-Fock) method to predict an intense band near 318 nm corresponding to the electronic excitation $(\sigma)^2(\sigma^*)^1 \rightarrow (\sigma)^1(\sigma^*)^2$, in which the N−Cl bonding is of the two-center-three-electron (2c-3e) orbital type with occupancy $(\sigma)^2(\sigma^*)^1$. Abu-Raqabah and Symons studied C_5H_5N−Cl radical in a $CFCl_3$ matrix at 77 K using electron paramagnetic resonance and established that this adduct has a three-electron bond unit with the chlorine atom lying in the plane of the ring.[12] To our knowledge, no infrared (IR) spectrum of the products of Cl + pyridine has been reported.

McKee *et al.* employed various quantum-chemical calculations to investigate adducts between Cl atom and a series of N-containing molecules and confirmed the (2c-3e) bond for all chlorine adducts investigated.[13] Hao *et al.* conducted B3LYP/3-21G* calculations on the chlorination mechanism of pyridine and reported that the barrier for formation of 2-chloropyridine + H is the lowest among three Cl-substitution paths.[14] Parveen *et al.* employed hybrid density-functional methods to find that formation of the C_5H_5N–Cl adduct with exothermicity of 52 kJ mol^{-1} is the primary channel at low temperature.[15] Although all three channels for addition of the Cl atom to the ring-carbon sites are predicted to have no barrier, the predicted ΔG values are positive even at 200 K; these ring additions are thus unlikely to contribute to the reaction unless the temperature is much less than 200 K. At high temperature, H-abstraction from the *ortho* C−H bond becomes feasible.[15]

Zhao *et al.* investigated the kinetics of the gaseous reaction Cl + C_5H_5N using laser flash photolysis and resonance fluorescence and found that H-abstraction is the dominant channel above 299 K, whereas in the temperature range 216−270 K the formation of an adduct is the major reaction channel as indicated by a pressure-dependent rate coefficient much greater than that for H-abstraction.[16] Equilibrium

a)Author to whom correspondence should be addressed. Electronic mail: yplee@mail.nctu.edu.tw.

constants for adduct formation and dissociation, determined from the forward and reverse rate coefficients, yield $\Delta H^{\circ}_{298} = 47.2 \pm 2.8$ kJ mol^{-1}. This experimental value of ΔH°_{298} is consistent with that predicted quantum-chemically for the formation of a planar adduct with a N−Cl σ-bond.[13,15]

The matrix isolation technique is an excellent method to investigate IR spectra of reactive intermediates.[17,18] Because of the cage effect that inhibits the Cl from escaping from the original cage upon photolysis of its precursor such as Cl_2, photolytic reactions of Cl atom in noble-gas matrices are ineffective. Taking advantage of the diminished matrix cage effect of p-H_2, Raston and Anderson produced isolated Cl atoms by photodissociation at 355 nm of Cl_2 trapped in solid p-H_2.[19] We have employed this method to investigate reactions of Cl with molecules including CS_2, C_2H_2, C_2H_4, C_3H_6, *trans*-1,3-butadiene, and C_6H_6 in p-H_2 to identify radicals ClSCS,[20] 1-chloroethyl ($\cdot CHClCH_3$),[21] 2-chloropropyl ($\cdot CH_2CHClCH_3$),[22] 2-chloroethyl ($\cdot CH_2CH_2Cl$),[23] and *trans*-1-chloromethylallyl [$\cdot(CH_2CHCH)CH_2Cl$][24] that were difficult to produce in typical experiments either in the gaseous phase or in noble-gas matrices.

In this work, we extended the investigations to the reaction of Cl with pyridine and report IR absorption spectra of the 1-chloropyridinyl (C_5H_5N−Cl) radical produced from addition of Cl to pyridine selectively onto the N-site.

II. EXPERIMENTS

The details of the p-H_2 matrix isolation apparatus have been described in Refs. 21 and 22. In brief, a gold-plated copper block, maintained at 3.2 K with a closed-cycle refrigerator system (Janis RKD-415), served as both a cold substrate for the matrix and a mirror to reflect the incident IR beam to the detector. The C_5H_5N/p-H_2 (1/3000−1/3200) mixture and Cl_2 were co-deposited over a period of 8−11 h. The flow rate of the C_5H_5N/p-H_2 mixture was maintained at 10−12 mmol h^{-1} and the flow rate of Cl_2 was maintained at 3−4 μmol h^{-1} to achieve a molar ratio of Cl_2:C_5H_5N:p-$H_2 \cong$ 3:1:3200.

After deposition the matrix was typically annealed at 4.5 K for 5 min to enhance the production of a complex between Cl_2 and C_5H_5N. To produce Cl atoms for reaction with C_5H_5N, we irradiated the matrix with ultraviolet light at 365 ± 10 nm from a light-emitting diode (Honle UV Technology, 375 mW) for 3 h. Following the photolysis at 365 nm, the matrix was annealed to 5.1 K for 3 min to induce further reaction.

Infrared absorption spectra were recorded with a Fourier-transform infrared FTIR spectrometer (Bomem, DA8) equipped with a KBr beam splitter and a HgCdTe detector cooled to 77 K. Interferograms were averaged over 600 scans to yield spectra in the range 400−4000 cm^{-1} at spectral resolution 0.25 cm^{-1}. Because excitation of the solid p-H_2 with IR light in the range 4000–5000 cm^{-1} induces reactions of Cl atoms with p-H_2 to form HCl,[25,26] we placed an IR filter with truncation wavelength at 2.4 μm (Andover Co.) before the entrance window of the matrix system for IR beam during acquisition of spectral data so as to avoid the reaction of Cl with H_2.

To confirm the observation of the C_5H_5N−HCl complex as a product, in a separate experiment, we co-deposited C_5H_5N/p-H_2 and HCl/p-H_2 mixtures at 3.2 K and record the IR spectra. Before deposition, gaseous HCl was prepared in a separate flask containing a mixture of Cl_2/p-H_2 (1/2400) by irradiation with light at 365 nm to initiate the reaction $Cl_2 + H_2 \rightarrow 2$ HCl.

Para-H_2 was synthesized by catalytic conversion of normal H_2 at low temperature. In this method, n-H_2 (99.999%, Scott Specialty Gases) was passed through a trap at 77 K and a copper coil filled with $Fe(OH)_3$ catalyst (catalyst grade, 30-50 mesh, Sigma-Aldrich) that was cooled with a closed-cycle refrigerator (Advanced Research System, DE204AF). The efficiency of conversion was controlled by the temperature of the catalyst. At conversion temperature 12−13 K, the concentration of o-H_2 is less than 100 ppm according to the Boltzmann distribution. Cl_2 (99.9%, Air Products and Chemicals) was used without further purification. Pyridine (Sigma-Aldrich, 99.8%) was distilled over KOH and degassed for several minutes to remove possible impurities.

III. COMPUTATIONAL METHOD

To characterize the complexes between C_5H_5N and Cl_2 molecules and to identify possible reaction products between Cl atom and C_5H_5N, the equilibrium structures, vibrational wavenumbers, IR intensities, and energies of possible products were calculated with the GAUSSIAN 09 program.[27] We employed the B3PW91 density-functional theory, which includes the three-parameter hybrid exchange functional of Becke[28] and gradient-corrected correlation functional of Perdew and Wang.[29] The McLean-Chandler basis sets for second-row atoms including p, d, and diffuse functions, designated 6-311++G(2d, 2p), were used.[30] Analytic first and second derivatives were applied for geometry optimization and vibrational wavenumbers at each stationary point. The anharmonic effects were calculated with a second-order perturbation approach using an effective finite-difference evaluation of the third and semidiagonal fourth derivatives.

A. σ- and π-bonded complexes of C_5H_5N–Cl_2

The structural parameters of σ- and π-bonded C_5H_5N–Cl_2 complexes, C_5H_5N, and Cl_2, optimized with the B3PW91/6-311++G(2d, 2p) method are shown in Fig. 1; those predicted previously with the MP2/aug-cc-pVDZ method[31] are listed parenthetically. These structures are consistent with reported structures except the position of the Cl_2 molecule in the π-bonded C_5H_5N–Cl_2 complex. Wang *et al.*[31] found that Cl_2 points towards the center of the C=C double bond in the π-bonded C_5H_5N–Cl_2 complex, whereas our results indicate that it points towards the *meta*-carbon atom of C_5H_5N at 99.6° with respect to the molecular plane of pyridine. According to their calculations of CCSD(T)/aug-cc-pVDZ using the full counterpoise method to correct for the effect of basis-set superposition error, the most stable structure of the C_5H_5N–Cl_2 complex is a σ-bonded planar structure with energy −16.8 (−32.5 before correction) kJ mol^{-1} relative to $Cl_2 + C_5H_5N$. The π-complex is predicted to be −5.6 (−15.4 before correction) kJ mol^{-1} relative to $Cl_2 + C_5H_5N$. Our values of −27.9 and

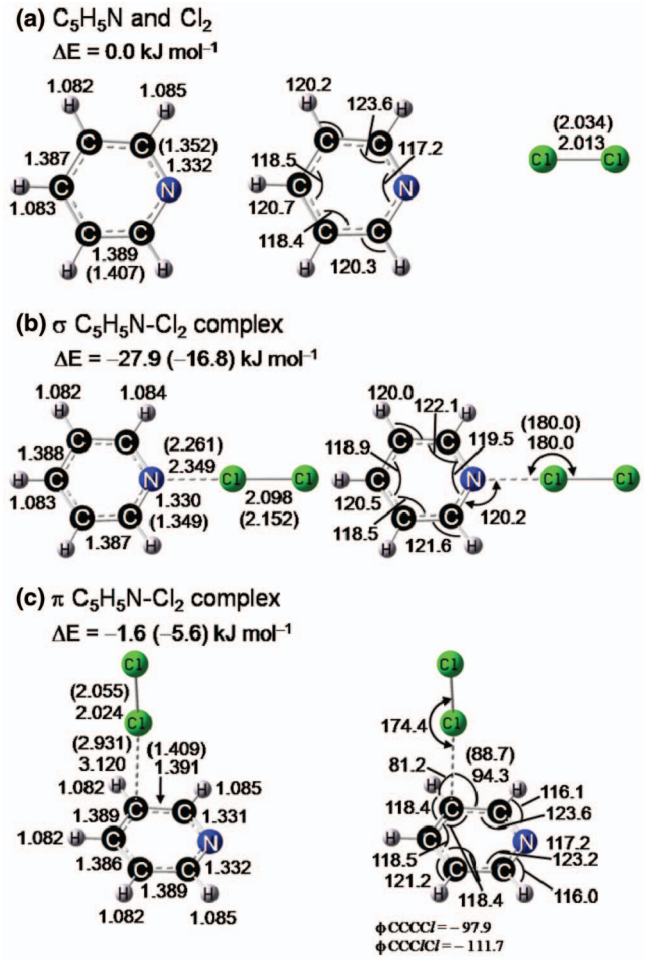

FIG. 1. Geometries and relative energies (in kJ mol^{-1}, zero-point energy corrected) of (a) C_5H_5N + Cl_2, (b) σ-C_5H_5N–Cl_2, and (c) π-C_5H_5N–Cl_2 optimized with the B3PW91/6-311++G(2d, 2p) method. Bond distances are in Å and bond angles in degrees. Reported parameters predicted with the MP2/aug-cc-pPVDZ method (Ref. 31) are listed in parentheses.

−1.6 kJ mol^{-1} for the σ- and π-complex of C_5H_5N–Cl_2, respectively, show a similar trend.

The N−Cl distance in the σ-complex of C_5H_5N–Cl_2 is 2.349 Å, consistent with the literature value of 2.261 Å; the distance between Cl and the pyridine plane in the π-complex was reported to be 2.931 Å.[31] At the B3PW91/6-311++G(2d, 2p) level of theory, the anharmonic vibrational wavenumbers for σ-bonded C_5H_5N–Cl_2 with IR intensities greater than 30 km mol^{-1} are predicted to be near 1598, 1455, 1217, 1075, 1014, 752, 697, 625, and 425 cm^{-1}, whereas those of π-bonded C_5H_5N–Cl_2 are near 1589, 1446, 704, and 525 cm^{-1}. A complete list of harmonic and anharmonic vibrational wavenumbers of both complexes appears in Table I.

The spectral pattern of the predicted IR spectrum of π-bonded C_5H_5N–Cl_2 is similar to that of C_5H_5N in terms of line positions and relative IR intensities except a new line near 525 cm^{-1} that is due to the Cl−Cl stretching mode. In contrast, the predicted lines of σ-bonded C_5H_5N–Cl_2 show larger shifts from those of C_5H_5N and a Cl−Cl stretching mode near 425 cm^{-1}, with an intensity pattern distinct from that of C_5H_5N.

B. 1-chloropyridinyl (C_5H_5N−Cl) radical

The 1-chloropyridinyl (C_5H_5N−Cl) radical was calculated to be the most stable isomer from Cl + C_5H_5N, with a stabilization energy of ∼52 kJ mol^{-1} (Ref. 15) that is consistent with the experimental result of $\Delta H^\circ_{298} = 47.2 \pm 2.8$ kJ mol^{-1}.[16] The geometry of the C_5H_5N−Cl radical computed with the B3PW91/6-311++G(2d, 2p) method is shown in Fig. 2(a). This geometry is similar to that predicted using the UMP2(full)/6-31G(d)[13] and the BB1K/6-31+G(d, p) methods;[15] parameters of the latter are shown in parentheses for comparison. The N−Cl bond distance, 2.366 Å, is

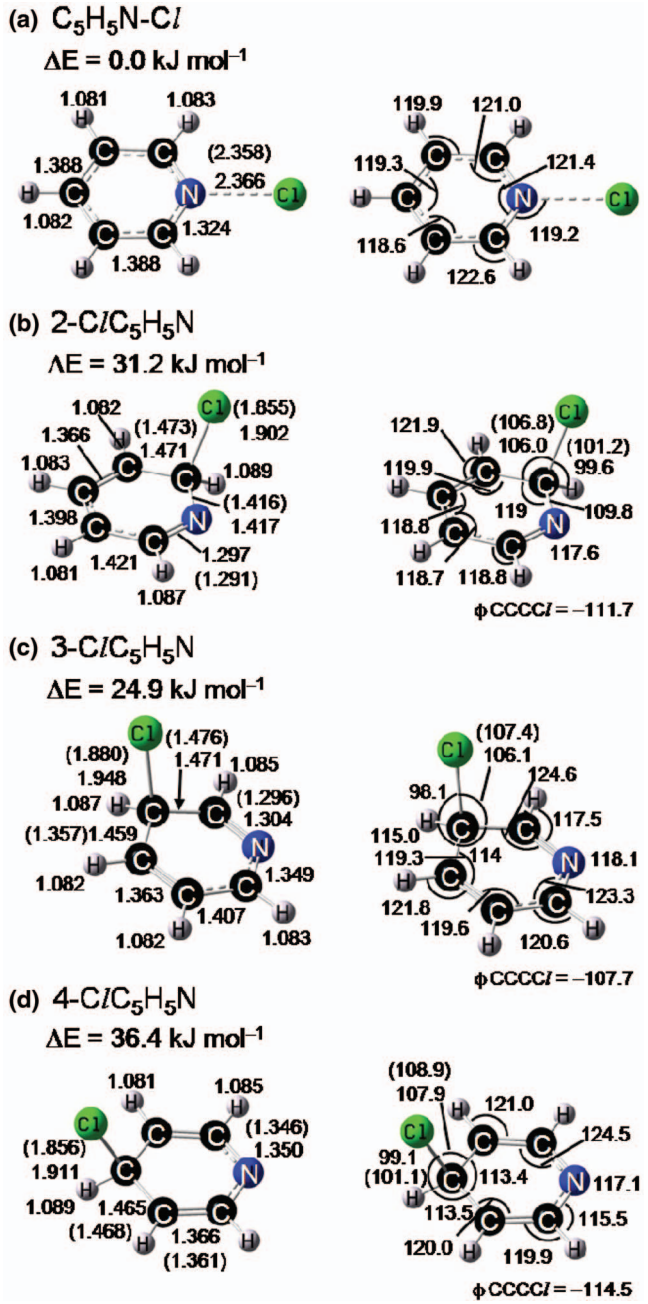

FIG. 2. Geometries and relative energies (in kJ mol^{-1}, zero-point energy corrected) of (a) C_5H_5N−Cl, (b) 2-ClC_5H_5N, (c) 3-ClC_5H_5N, and (d) 4-ClC_5H_5N optimized with the B3PW91 / 6-311++G(2d, 2p) method. Bond lengths are in Å and bond angles in degrees. Reported parameters predicted with the BB1K/6-31+G(d,p) method (Ref. 15) are listed in parentheses.

TABLE I. Comparison of observed vibrational wavenumbers (in cm^{-1}) and relative IR intensities of C_5H_5N and σ-bonded C_5H_5N–Cl_2 complex with harmonic and anharmonic vibrational wavenumbers and relative IR intensities of C_5H_5N, σ- and π-bonded C_5H_5N–Cl_2 complexes predicted with the B3PW91/6-311++G(2d, 2p) method.

			B3PW91/6-311++G(2d, 2p)					
	p-H_2		C_5H_5N		σ-C_5H_5N–Cl_2 [c]		π-C_5H_5N–Cl_2 [c]	
Mode[a]	C_5H_5N [b]	σ-C_5H_5N–Cl_2	Harmonic	Anharmonic	Harmonic	Anharmonic	Harmonic	Anharmonic
	3093.0 (6.9)[d]							
ν_1	3084.6 (27.4)	3091.4 (14.9)[d]	3200 (30.4)[d]	3070	3210 (13.8)[d]	3082	3201 (16.4)[d]	3069
ν_2	3086.3 (16.8)	3070.5 (3.7)	3207 (8.3)	3064	3216 (16.2)	3073	3209 (5.3)	3062
ν_3	3063.9 (8.7)		3183 (6.0)	3051	3194 (0.0)	3063	3187 (3.1)	3049
	3058.1 (8.6)							
ν_4	3039.0 (28.5)	3047.2 (9.3)	3158 (38.0)	3032	3183 (6.6)	3064	3161 (24.6)	3021
ν_5	3030.2 (14.5)	3018.5 (9.3)	3160 (5.2)	3015	3184 (10.3)	3011	3164 (5.0)	3011
	3007.0 (22.9)							
	1598.5 (28.5)							
ν_6	1582.9 (43.9)	1591.8 (66.9)	1635 (34.8)	1590	1642 (34.2)	1598	1632 (40.6)	1589
ν_7	1579.5 (15.3)	1581.3 (11.4)	1631 (14.7)	1589	1634 (8.3)	1593	1628 (20.3)	1586
ν_8	1483.2 (12.5)		1518 (3.9)	1488	1518 (1.2)	1486	1517 (4.4)	1486
ν_9	1440.8 (48.8)	1446.7 (74.9)	1476 (39.6)	1447	1483 (50.6)	1455	1475 (31.1)	1446
ν_{10}			1384 (0.1)	1356	1378 (2.0)	1354	1385 (0.1)	1354
ν_{11}			1302 (0.0)	1253	1314 (2.6)	1265	1303 (0.4)	1256
ν_{12}	1217.7 (13.2)	1212.7 (27.3)	1243 (5.7)	1225	1234 (31.4)	1217	1243 (6.2)	1224
ν_{13}	1144.3 (10.5)	1147.6 (8.2)	1167 (3.7)	1153	1173 (4.3)	1158	1169 (3.9)	1154
ν_{14}	1071.1 (10.3)	1070.3 (30.4)	1096 (6.5)	1075	1096 (38.4)	1075	1096 (4.5)	1076
ν_{15}			1081 (0.0)	1056	1090 (0.8)	1060	1079 (1.2)	1053
ν_{16}	1031.9 (23.6)	1030.4 (12.3)	1052 (8.0)	1035	1048 (0.0)	1032	1051 (10.1)	1034
ν_{17}			1014 (0.0)	1010	1021 (0.0)	1000	1011 (2.7)	1005
ν_{18}	991.3 (11.9)	1003.7 (46.8)	1014 (8.7)	999	1031 (32.0)	1014	1014 (4.9)	1000
ν_{19}			1004 (0.0)	999	1007 (0.0)	986	1004 (1.0)	993
ν_{20}			959 (0.0)	946	966 (0.0)	945	958 (0.1)	943
ν_{21}			892 (0.0)	885	891 (0.0)	879	893 (5.3)	886
ν_{22}	744.2 (35.0)	746.2 (42.1)	764 (9.2)	753	767 (30.0)	752	767 (16.3)	752
ν_{23}	701.6 (100.0)	699.0(100.0)	715 (100)	706	712 (100)	697	715 (100)	704
ν_{24}			667 (0.3)	660	662 (0.1)	655	666 (0.2)	660
ν_{25}	601.8 (13.9)	616.2 (42.9)	613 (5.9)	606	632 (36.6)	625	611 (4.6)	604
ν_{26}			415 (5.4)	407	431 (4.9)	415	415 (2.5)	406
Cl−Cl		458.4 (188.7)			422 (370)	425	534 (30.8)	525
ν_{27}			378 (0.0)	373	387 (0.0)	376	377 (0.3)	371

[a]The order of modes follows the predicted anharmonic vibrational wavenumbers of C_5H_5N.
[b]The assignments in the 3000−3100 cm^{-1} region are tentative. Observed additional lines are due to overtone or combination bands.
[c]Additional modes are predicted to have harmonic (relative IR intensity)/anharmonic vibrational wavenumbers (in cm^{-1}): 207 (0.2)/194, 184 (0.0)/168, 114 (79)/105, 52 (0.0)/36, and 51 (0.6)/43 for σ-C_5H_5N–Cl_2 and 69 (1)/54, 55 (1.4)/47, 53 (0.3)/40, 26 (0.5)/35, and 23 (2.6)/32 for π-C_5H_5N–Cl_2.
[d]Percentage IR intensities relative to the intense line near 700 cm^{-1} are listed in parentheses. IR intensities of the lines near 700 cm^{-1} of C_5H_5N, σ-C_5H_5N–Cl_2, and π-C_5H_5N–Cl_2 are predicted to be 68.2, 58.8, and 82.9 km mol^{-1}, respectively.

similar to the corresponding value in the σ−bonded C_5H_5N–Cl_2 complex. The anharmonic vibrational wavenumbers for modes of C_5H_5N−Cl with IR intensities greater than 15 km mol^{-1} are predicted to be near 3067, 1455, 1206, 1001, 748, and 692 cm^{-1}. Harmonic and anharmonic vibrational wavenumbers of C_5H_5N−Cl are listed in Table II.

C. 2-, 3-, and 4-chloropyridinyl (ClC_5H_5N) radicals

The geometries of 2-, 3-, and 4-chloropyridinyl (ClC_5H_5N) radicals computed with the B3PW91/6-311++G(2d, 2p) method are shown in Figs. 2(b)–2(d). Although the C−Cl bond distances, 1.902−1.948 Å, of these radicals are smaller than the N−Cl bond length of 2.366 Å in C_5H_5N−Cl, the energies of 2-, 3-, and 4-ClC_5H_5N are 31, 25, and 36 kJ mol^{-1} greater than that of C_5H_5N−Cl, presumably because the σ-bond between the Cl and the C atoms suppresses the aromaticity. Parveen and Chandra reported that ΔH for formation of 2-, 3-, and 4-ClC_5H_5N are 32, 27, and 37 kJ mol^{-1} larger than that of C_5H_5N−Cl,[15] in agreement with our results. The harmonic and anharmonic vibrational wavenumbers of 2-, 3-, and 4-ClC_5H_5N radicals are listed in Table II. According to calculations, the C−Cl stretching modes are predicted to be near 282, 210, and 270 cm^{-1} for 2-, 3-, and 4-ClC_5H_5N, respectively, beyond our detection range. The most intense lines are predicted near 743, 752, and 756 cm^{-1} for 2-, 3-, and 4-ClC_5H_5N, respectively; they are about 50 cm^{-1} greater than the wavenumber of the corresponding line of C_5H_5N−Cl near 692 cm^{-1}.

TABLE II. Comparison of observed vibrational wavenumbers (in cm^{-1}) and relative IR intensities of C_5H_5N-Cl with harmonic and anharmonic vibrational wavenumbers and relative IR intensities of C_5H_5N-Cl, 2-, 3-, and 4-ClC_5H_5N predicted with the B3PW91/6-311++G(2d, 2p) method.

		B3PW91/6-311++G(2d, 2p)							
	p-H_2	C_5H_5N-Cl		2-ClC_5H_5N		3-ClC_5H_5N		4-ClC_5H_5N	
Mode[a]	C_5H_5N-Cl[b]	Harmonic	Anharmonic	Harmonic	Anharmonic	Harmonic	Anharmonic	Harmonic	Anharmonic
ν_1	3075.9 (18.9)[c]	3189 (9.6)	3088	3215 (4.3)[c]	3085	3211 (8.0)[c]	3071	3211 (0.5)[c]	3086
ν_2	3064.1 (?)	3211 (11.0)	3084	3208 (5.4)	3076	3196 (21.2)	3068	3210 (10.6)	3082
ν_3		3199 (3.8)	3077	3188 (3.2)	3059	3182 (4.3)	3055	3172 (3.8)	3041
ν_4		3193 (0.5)	3069	3140 (19.8)	3008	3165 (18.1)	3037	3169 (31.7)	3038
ν_5	3058.3 (?)	3217 (17.9)[c]	3067	3096 (1.4)	2944	3126 (1.5)	2981	3092 (0.9)	2942
ν_6		1637 (8.2)	1594	1588 (4.3)	1542	1583 (23.8)	1556	1574 (8.8)	1544
ν_7		1631 (1.3)	1580	1546 (14.4)	1505	1539 (21.4)	1500	1489 (39.4)	1454
ν_8		1511 (2.9)	1480	1439 (9.3)	1408	1460 (51.2)	1430	1462 (13.8)	1432
ν_9	1449.7 (59.4)	1484 (57.0)	1455	1419 (17.9)	1393	1397 (32.2)	1371	1429 (15.0)	1401
ν_{10}	1354.4 (4.1)	1367 (3.9)	1343	1365 (0.7)	1334	1374 (0.0)	1347	1352 (2.3)	1323
ν_{11}		1320 (7.8)	1299	1327 (2.7)	1292	1299 (7.3)	1277	1221 (0.2)	1201
ν_{12}	1200.6 (16.1)	1224 (15.1)	1206	1181 (3.7)	1159	1189 (9.9)	1170	1178 (38.5)	1150
ν_{13}	1148.8 (6.4)	1173 (4.4)	1158	1154 (3.4)	1120	1171 (4.3)	1156	1151 (0.0)	1133
ν_{14}	1069.3 (16.2)	1097 (13.3)	1075	1133 (6.3)	1111	1126 (3.8)	1077	1129 (3.8)	1092
ν_{15}		1087 (1.1)	1058	1060 (5.1)	1031	1057 (4.3)	1040	1062 (3.6)	1044
ν_{16}		1044 (0.6)	1028	1017 (19.2)	999	1039 (6.7)	1025	1042 (0.2)	1020
ν_{17}		1019 (0.1)	1004	1006 (5.2)	987	1002 (31.1)	986	989 (0.6)	976
ν_{18}	1017.4 (5.5)	1016 (17.8)	1001	979 (1.4)	968	975 (4.9)	968	989 (8.0)	969
ν_{19}		1000 (0.0)	987	974 (4.0)	961	904 (13.4)	892	974 (2.1)	954
ν_{20}		961 (0.1)	946	885 (7.3)	871	879 (14.9)	869	905 (4.2)	895
ν_{21}		883 (0.0)	873	813 (2.5)	805	851 (19.4)	838	791 (0.1)	778
ν_{22}	742.9 (58.1)	759 (49.4)	748	752 (100)	743	756 (100)	752	769 (100)	756
ν_{23}	688.7 (100)	704 (100)	692	662 (8.5)	655	655 (38.0)	646	670 (12.7)	650
ν_{24}		656 (0.3)	649	625 (12.0)	617	621 (7.3)	614	632 (9.0)	625
ν_{25}		630 (2.4)	623	587 (10.8)	576	583 (4.9)	577	583 (44.4)	575
ν_{26}		418 (5.6)	409	439 (23.6)	421	416 (37.2)	393	428 (10.9)	399
ν_{27}		386 (0.0)	380	400 (5.8)	384	341 (41.5)	321	393 (0.1)	383
ν_{28}		197 (1.0)	194	299 (30.4)	282	250 (145)	210	294 (58.6)	270
ν_{29}		89 (1.1)	93	220 (0.0)	218	198 (5.6)	193	204 (1.1)	201
ν_{30}		55 (0.0)	59	86 (0.9)	82	94 (1.9)	90	94 (4.4)	88

[a]The order of modes follows the predicted anharmonic vibrational wavenumbers.
[b]The assignments in the 3000−3100 cm^{-1} region are tentative. The '?' marks indicate that either the assignment or the relative intensity is uncertain because of the severe overlap with other lines.
[c]Percentage IR intensities relative to the most intense line near 750 cm^{-1} (700 cm^{-1} for C_5H_5N-Cl) are listed in parentheses. IR intensities of these lines are 52.4, 101.5, 46.2, and 75.4 km mol^{-1} for C_5H_5N-Cl, 2-, 3-, and 4-ClC_5H_5N, respectively.

D. 2-, 3-, and 4-pyridyl radicals (C_5H_4N)

Pyridyl (C_5H_4N) radicals might be produced via H-abstraction reaction of C_5H_5N by the Cl atom. The geometries of 2-, 3-, and 4-pyridyl radicals, predicted with the B3PW91/6-311++G(2d, 2p) method, are presented in Fig. S1 (supplementary material).[32] The 2-pyridyl radical is found to be the most stable of the three pyridyl radicals, consistent with reported findings.[33–35] The barrier for the Cl + C_5H_5N abstraction to produce 2-, 3-, and 4-C_5H_4N was predicted to be 13, 44, and 37 kJ mol^{-1}, respectively, with the BB1K/6-31+G(d,p) method.[15] The anharmonic vibrational wavenumbers for modes of 2-C_5H_4N with IR intensities greater than 20 km mol^{-1} are predicted to be near 3044, 1619, 1556, 1397, 1054, 942, 739, and 570 cm^{-1} with the B3PW91/6-311++G(2d, 2p) method. A complete list of the harmonic and anharmonic vibrational wavenumbers and relative IR intensities predicted for 2-, 3-, and 4-pyridyl radicals is available in supplementary material (Table SI).[32]

IV. EXPERIMENTAL RESULTS

A. Formation of the C_5H_5N–Cl_2 complex in p-H_2

The IR spectrum of C_5H_5N in p-H_2 (1/3200) at 3.2 K in the spectral regions 420−780, 980−1280, 1400−1620, and 2980−3140 cm^{-1} is presented in Fig. 3(a). It contains intense lines at 3084.6, 3039.0, 3007.0, 1598.5, 1582.9, 1579.5, 1483.2, 1440.8, 1217.7, 1031.9, 991.3, 744.2, 701.6, and 601.8 cm^{-1}; a complete list is included in Table I. These line positions are in agreement with those of gaseous C_5H_5N (Ref. 36) and C_5H_5N isolated in N_2 (Ref. 37) and Ar matrices[38] reported previously.

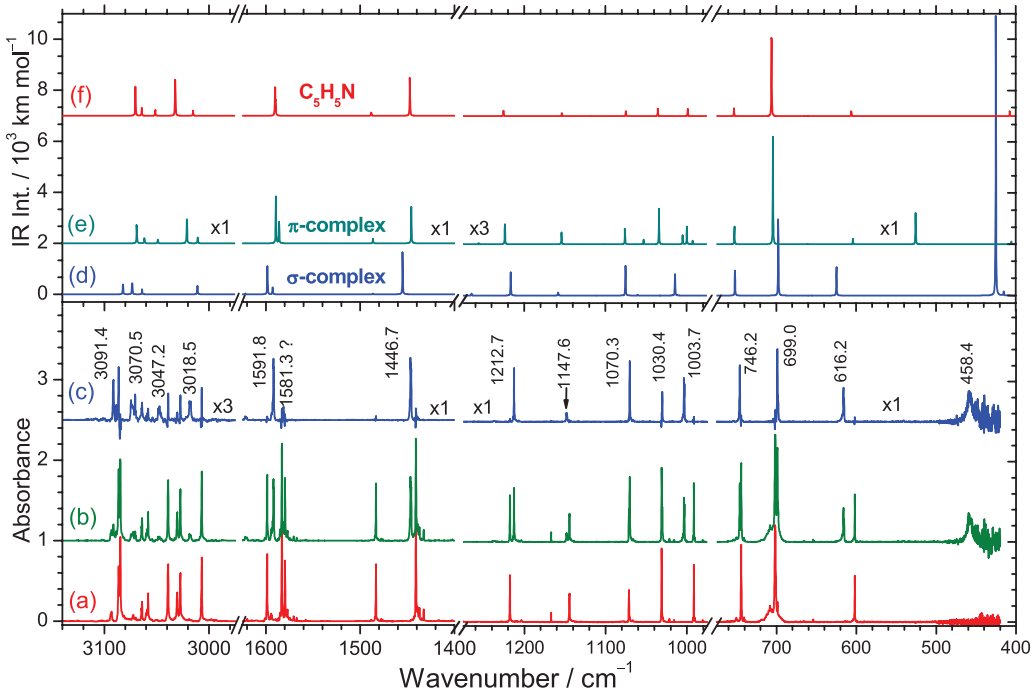

FIG. 3. (a) Absorption spectrum of a $C_5H_5N/p\text{-}H_2$ (1/3200) matrix deposited at 3.2 K for 11 h. (b) Absorption spectrum of a $Cl_2/C_5H_5N/p\text{-}H_2$ (3/1/3200) matrix deposited at 3.2 K for 11 h and annealed at 4.5 K for 5 min. (c) Difference spectrum of (b) − 0.94×(a). (d) IR stick spectrum simulated according to anharmonic vibrational wavenumbers and IR intensities of σ-C_5H_5N–Cl_2 predicted with the B3PW91/6-311++G(2d, 2p) method. (e) Simulated stick spectrum of π-C_5H_5N–Cl_2, and (f) simulated stick spectrum of C_5H_5N. All experimental spectra were recorded at resolution 0.25 cm^{-1}.

When a mixture of $Cl_2/C_5H_5N/p\text{-}H_2$ (3/1/3200) was deposited at 3.2 K, new lines appear; their intensities increase upon annealing to 4.5 K for 5 min, as shown in Fig. 3(b). For clarity in showing the new lines induced by the presence of Cl_2, we stripped lines due to isolated C_5H_5N (Fig. 3(a)) from the spectrum in Fig. 3(b) to yield the difference spectrum in Fig. 3(c). These new features with intense ones at 3091.4, 3047.2, 1591.8, 1446.7, 1212.7, 1070.3, 1003.7, 746.2, 699.0, 616.2, and 458.4 cm^{-1} are assigned to the σ-bonded C_5H_5N–Cl_2 complex, to be discussed in Sec. V A. A complete list of vibrational wavenumbers and relative IR intensities of these new features is presented in Table I. If we assume that the predicted IR intensities of C_5H_5N and C_5H_5N–Cl_2 are reliable, we estimate that, according to Fig. 3(b), the mixing ratio of $[C_5H_5N]$:$[C_5H_5N–Cl_2]$ is approximately 1.0:0.6.

B. Photolysis of $Cl_2/C_5H_5N/p\text{-}H_2$ matrices

Upon irradiation of a $Cl_2/C_5H_5N/p\text{-}H_2$ matrix with light at 365 nm, the intensities of IR lines due to C_5H_5N and C_5H_5N–Cl_2 complexes decreased, and new features in several groups appeared. These features are expected to result from reactions between Cl atom and C_5H_5N. A difference spectrum obtained on subtracting the spectrum of a $Cl_2/C_5H_5N/p\text{-}H_2$ (3/1/3200) matrix recorded upon deposition, followed by annealing at 4.5 K for 5 min and irradiation with 365 nm light for 3 h, from that recorded after subsequent annealing at 5.1 K for 3 min is presented in Fig. 4(b); lines pointing upwards indicate production; downward lines due to destruction of the precursors are suppressed. For comparison, the spectrum of a $Cl_2/C_5H_5N/p\text{-}H_2$ (3/1/3200) matrix recorded upon deposition at 3.2 K for 11 h followed by annealing at 4.5 K for 5 min is shown in Fig. 4(a). In the difference spectrum shown in Fig. 4(b), several lines of C_5H_5N and C_5H_5N–Cl_2 show first-derivative shapes because of small shifts in line positions and changes in line shape upon photolysis and annealing.

As the IR intensities of new features remained small even after prolonged irradiation we deduced that the photoproducts underwent further photodecomposition. The greatest intensity of new features was attained upon annealing. To illustrate this condition, we show a difference spectrum obtained on subtracting the spectrum in Fig. 4(b) from that recorded upon further irradiation of the matrix at 365 nm for 12 min. Lines at 3075.9, 1449.7, 1200.6, 1148.8, 1069.3, 1017.4, 742.9, and 688.7 cm^{-1} were produced upon annealing following 365-nm irradiation (upward pointing in Fig. 4(b)), but decreased in intensity upon further irradiation at 365 nm (downward pointing in Fig. 4(c)). These lines are denoted group A and indicated with "A" in Fig. 4. In the CH-stretching region, because of the severe overlap with absorption lines of the precursors, only one intense line is clearly identified at 3075.9 cm^{-1}. Two additional lines at 3058.3 and 3064.1 cm^{-1} might also belong to the same group, because they show a similar trend (upward in Fig. 4(b) and downward in Fig. 4(c)), but parent absorption might interfere with the intensity ratios in these traces. These lines in group A are assigned to the 1-chloropyridinyl (C_5H_5N−Cl) radical, to be discussed in Sec. V B. The vibrational wavenumbers and relative IR intensities of these new features are listed in Table II.

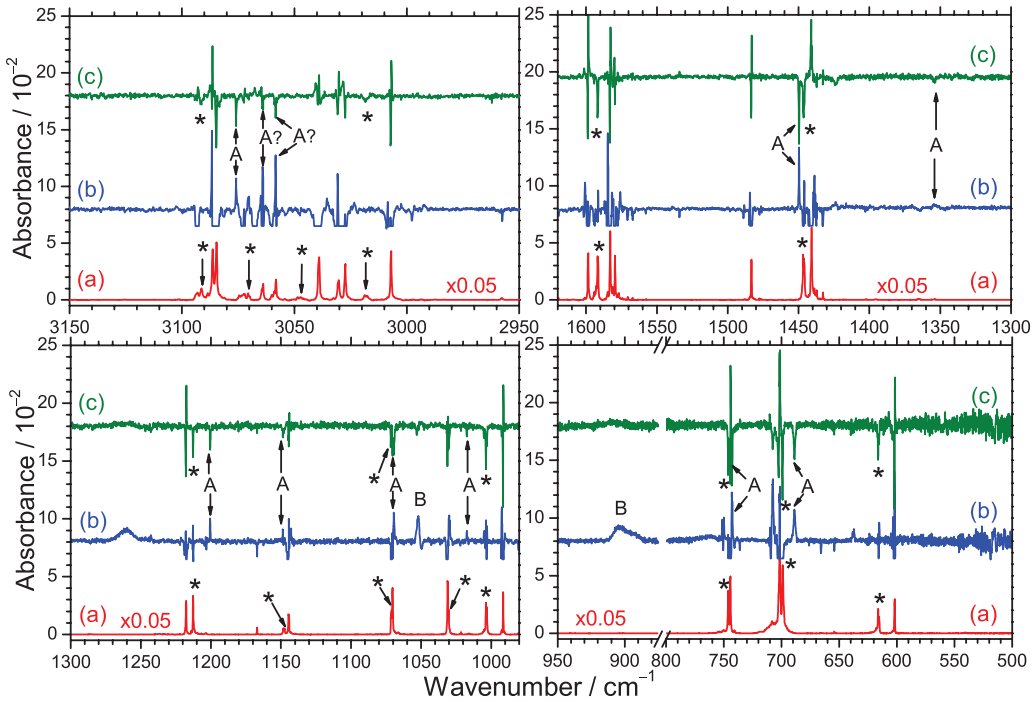

FIG. 4. (a) Absorption spectrum of a $Cl_2/C_5H_5N/p\text{-}H_2$ (3/1/3200) matrix deposited at 3.2 K for 11 h and annealed at 4.5 K for 5 min. (b) Difference spectrum of the matrix after irradiation at 365 nm for 3 h, followed by annealing at 5.1 K for 3 min. (c) Difference spectrum of the matrix after further photolysis at 365 nm for 12 min. All experimental spectra were recorded at resolution 0.25 cm^{-1}. Lines marked with "*" are assigned to the σ-C_5H_5N–Cl_2 complex. Lines marked with "A" and "B" are assigned to C_5H_5N−Cl and C_5H_5N–HCl complex, respectively.

When we assume that the predicted IR intensities of C_5H_5N, C_5H_5N–Cl_2, and C_5H_5N−Cl are correct, we estimate the variation in mixing ratios $\Delta[C_5H_5N]$:$\Delta[C_5H_5N$-$Cl_2]$:$\Delta[C_5H_5N$−Cl] to be approximately $-(1.0 \pm 0.4)$: $-(0.05 \pm 0.01)$:(0.07 ± 0.01) after annealing (Fig. 4(b)) and $\Delta[C_5H_5N]$:$\Delta[C_5H_5N$–$Cl_2]$:$\Delta[C_5H_5N$−Cl] to be approximately $\sim-(1.0 \pm 0.4)$:$-(0.27 \pm 0.05)$:$-(0.43 \pm 0.02)$ after secondary photolysis (Fig. 4(c)). Some C_5H_5N might have evaporated upon annealing.

Lines in a second group, produced after photolysis and further increased in intensity upon annealing at 5.1 K, showed little change in intensity upon further irradiation at 365 nm, and are indicated with "B" in Fig. 4(b) and termed group B. Lines in group B include a broad feature near 904.5 cm^{-1} and a line near 1052.1 cm^{-1}. Barnes *et al.* reported intense lines at 840 and 1050 cm^{-1} and assigned them to the antisymmetric stretching and bending modes of the N−H−Cl moiety of C_5H_5N–HCl in solid Ar, respectively.[39] Subsequent experiments confirmed this experimental result and reported lines at 1491.0, 1072.0, 1051.0, and 838.0 cm^{-1} for C_5H_5N–HCl in solid Ar.[40–42] To confirm the assignment, a separate experiment in which C_5H_5N and HCl were co-deposited with $p\text{-}H_2$ ($C_5H_5N/HCl/p\text{-}H_2$ = 1/1/2400) at 3.2 K, as shown in Fig. S2 (supplementary material).[32] Lines at 1491.8, 1455.4, 1066.4, 1052.3, and 904.5 cm^{-1} are assigned to C_5H_5N–HCl in solid $p\text{-}H_2$. As the two intense lines in group B are nearly identical to those observed for C_5H_5N–HCl in a $p\text{-}H_2$ matrix, we assigned these features to the C_5H_5N–HCl complex.

V. DISCUSSION

A. Assignment of lines of the σ-bonded C_5H_5N–Cl_2 complex

There is no report of identification of C_5H_5N–Cl_2 complexes with IR spectra, but Kimel'fel'd *et al.* reported Raman spectra of Cl_2 and Br_2 complexes with several amines including C_5H_5N at 77 K; a broad line at 440 cm^{-1} was reported for C_5H_5N–Cl_2.[43] Rubenacker *et al.* measured nuclear-quadrupole-resonance spectra of pyridine-halogen complexes including C_5H_5N–Cl_2 at 77 K and proposed that this complex is ionic.[44] As described in Sec. III A, the σ-bonded C_5H_5N–Cl_2 complex is more stable than the π-bonded complex. Wang *et al.* reported that, according to their calculations of ΔG, the formation of the σ-bonded C_5H_5N–Cl_2 complex but not the π-bonded complex is spontaneous at 200 K.[31]

Upon co-deposition of Cl_2 with pyridine in $p\text{-}H_2$, we observed many new features (Fig. 3(c)) as compared with the spectrum of $C_5H_5N/p\text{-}H_2$ at 3.2 K (Fig. 3(a)). The intensity of these lines increases significantly upon annealing, consistent with the expectation that these lines are due to the formation of a complex between C_5H_5N and Cl_2. The positions of most newly observed lines are similar to those of pyridine, but lines at 458.4, 616.2, and 1003.7 cm^{-1} are distinct from those of C_5H_5N.

For comparison, we plot the simulated IR spectra of σ-bonded C_5H_5N–Cl_2 complex, π-bonded C_5H_5N–Cl_2 complex, and C_5H_5N in Figs. 3(d) and 3(e); the

spectra were simulated according to the anharmonic vibrational wavenumbers and IR intensities predicted with the B3PW91/6-311++G(2d, 2p) method and a spectral width of 0.25 cm^{-1}. The wavenumbers of π-bonded C_5H_5N–Cl_2 are similar to those of C_5H_5N except an enhanced feature near 534 cm^{-1} that is associated with the Cl−Cl stretching vibrational mode. In contrast, the spectrum of σ-bonded C_5H_5N–Cl_2 shows more significant spectral shifts and two significantly enhanced features near 422 (Cl−Cl stretching mode) and 632 cm^{-1} (in-plane ring deformation mode).

Observed new features with intense ones at 3091.4, 1591.8, 1446.7, 1212.7, 1070.3, 1003.7, 746.2, 699.0, 616.2, and 458.4 cm^{-1} agree satisfactorily with lines predicted for the σ-bonded C_5H_5N–Cl_2 in both wavenumbers and relative intensities, as shown in Figs. 3(c) and 3(d). Relative to absorption lines of C_5H_5N, most lines are blueshifted, except lines at 1212.7, 1070.3, and 699.0 cm^{-1} that are redshifted, consistent with theoretical predictions of the direction of shifts (Table I). In the region below 500 cm^{-1} a unique broad feature at 458.4 cm^{-1} with full-width at half maximum (FWHM) of ~7.2 cm^{-1} was observed and is assigned to the Cl−Cl stretching mode of C_5H_5N–Cl_2; this mode was predicted to have harmonic (anharmonic) vibrational wavenumbers near 422 (425) cm^{-1}. That the width of this spectral line is much larger than that of other lines might indicate that a distribution of N−Cl−Cl angles is present in the complex. The assignments of some lines in the 3000−3100 cm^{-1} region are tentative because of the similarity in vibrational wavenumbers and large anharmonicity associated with these modes and possible interference from the combination bands. Some lines are missing because of the severe overlap with absorption lines of C_5H_5N. For lines below 2000 cm^{-1}, the average deviation between observed and predicted anharmonic vibrational wavenumbers is 8.9 cm^{-1}, with a maximum deviation of 33 cm^{-1} for the Cl−Cl stretching mode at 425 cm^{-1}.

Considering the agreement in positions and relative IR intensities between observed and predicted lines for the σ-bonded C_5H_5N–Cl_2 complex, the absence of a unique feature near 530 cm^{-1} predicted for the π-bonded complex, and the calculated thermochemistry, we assigned these new features to the σ-bonded C_5H_5N–Cl_2 complex.

B. Assignment of lines in group A to the 1-chloropyridinyl radical (C_5H_5N−Cl)

New lines in group A appeared upon annealing of a matrix of $Cl_2/C_5H_5N/p$-H_2 irradiated at 365 nm. Because photons at 365 nm dissociate only Cl_2 to produce Cl, not pyridine,[45] we expect that the species produced upon annealing result from the reaction of Cl and pyridine via a barrierless path. During photolysis the intensities of lines in group A remain small, attributed to secondary photolysis of C_5H_5N−Cl. This reaction is supported by the observation of diminished intensity after further irradiation of the annealed matrix for 12 min, as shown in Fig. 4(c).

Although the addition of Cl to the N-atom site of pyridine is predicted to be the only spontaneous process near 300 K, we cannot exclude the possibility that addition of Cl to the ring carbon atoms at 2-, 3-, and 4-positions occurs at 5 K.[15] The products of H-abstraction to form HCl + C_5H_4N, although unlikely to have a major contribution in the matrix near 3 K, should also be considered.

In Fig. 5(a) we reproduce the difference spectrum upon annealing at 5.1 K for 3 min of the $Cl_2/C_5H_5N/p$-H_2 (3.0/1.0/3200) matrix previously irradiated at 365 nm. Lines of group A are marked as "A" and the regions interfered by intense absorption of C_5H_5N and C_5H_5N–Cl_2 are marked with grey. In Figs. 5(b)–5(e) we plot the simulated IR spectra of radicals 1-chloropyridinyl (C_5H_5N−Cl), 2-, 3-, and 4-chloropyridinyl (ClC_5H_5N), respectively; the spectra were simulated according to the anharmonic vibrational wavenumbers and IR intensities predicted with the B3PW91/6-311++G(2d, 2p) method and a spectral width of 0.25 cm^{-1}. The spectra of all three isomers of ClC_5H_5N are distinct because the C−Cl bonding at various sites of carbon has distinct effects on the bonding of the carbon ring. The simulated spectrum of C_5H_5N−Cl most resembles the spectrum of C_5H_5N, presumably because the weak interaction of Cl with the lone pair of the N atom least perturbs the structure of pyridine.

The observed wavenumbers and relative intensities of lines are in satisfactory agreement with those calculated for the C_5H_5N−Cl radical, but not with any of the 2-, 3-, and 4-chloropyridinyl (ClC_5H_5N) radicals, as illustrated in Fig. 5 and listed in Table II. The three most intense lines were observed at 1449.7, 742.9, and 688.7 cm^{-1}, near those predicted at 1455 (coupled C−C stretching and C−H in-plane bending mode), 748 (C−H out-of-plane bending mode), and 692 cm^{-1} (C−H out-of-plane mode). The N−Cl stretching mode was predicted to be near 194 cm^{-1}, beyond our detection range. Assignments in the CH-stretching region are tentative because several modes were predicted to have similar vibrational wavenumbers and the anharmonicity correction altered the order of these modes. For lines below 2000 cm^{-1}, the average deviation between observed and predicted anharmonic vibrational wavenumbers is 7.2 cm^{-1}, with a maximum of 16.4 cm^{-1} for the in-plane ring deformation mode (ν_{18}) at 1017.4 cm^{-1}. The most intense line at 688.7 cm^{-1} has a width (FWHM) of 1.7 cm^{-1}, larger than for other lines of this species. One possible reason is that, according to the quantum-chemical calculations, this mode involves motion that changes the distance between N and Cl and perhaps the potential energy surface with respect to the N−Cl distance is relatively flat. These observed lines in group A do not match those predicted for any H-abstraction product 2- or 3- or 4-C_5H_4N either, as shown in Table SI (supplementary material).[32]

Considering the observed photolytic and annealing behavior, the agreement in wavenumber and relative IR intensity between lines observed and predicted for the C_5H_5N–Cl radical, the absence of some unique features of 2-, 3-, and 4-chloropyridinyl (ClC_5H_5N), and the calculated thermochemistry, we assign these new features in group A to the *N*-pyridinyl radical (C_5H_5N–Cl).

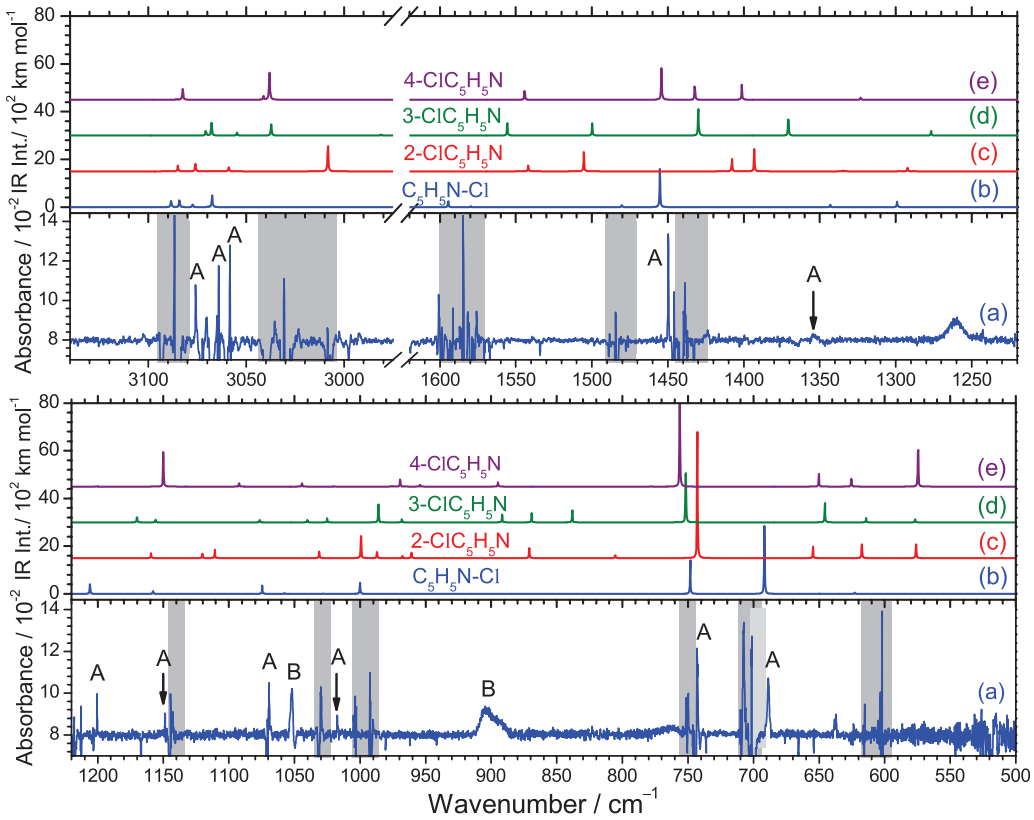

FIG. 5. (a) Difference spectrum of a $Cl_2/C_5H_5N/p\text{-}H_2$ (3/1/3200) matrix (deposited at 3.2 K for 11 h, annealed at 4.5 K for 5 min, and irradiated at 365 nm for 3 h) after annealing at 5.1 K for 3 min; lines of groups A and B are marked and regions interfered by C_5H_5N and C_5H_5N–Cl_2 are marked with light grey areas. (b) IR stick spectrum simulated according to anharmonic vibrational wavenumbers and IR intensities of C_5H_5N−Cl predicted with the B3PW91/6-311++G(2d, 2p) method. Simulated stick spectra of (c) 2-ClC_5H_5N, (d) 3-ClC_5H_5N, and (e) 4-ClC_5H_5N. All experimental spectra were recorded at resolution 0.25 cm^{-1}.

C. Reaction mechanisms in solid *p*-H_2

Upon irradiation of a $Cl_2/C_5H_5N/p\text{-}H_2$ matrix at 365 nm, the initial process is the dissociation of Cl_2 molecules to form Cl atoms. The production of isolated Cl atoms was confirmed with the observation of a line at 943.7 cm^{-1} associated with its spin-orbit transition $^2P_{1/2} \leftarrow {}^2P_{3/2}$, consistent with the report by Raston and Anderson.[19]

The Cl atoms might react with nearby C_5H_5N to form C_5H_5N−Cl or 2-, 3-, 4-ClC_5H_5N radicals; annealing of the matrix containing Cl and C_5H_5N enhances this reaction and avoids secondary photolysis. We observed C_5H_5N−Cl as the dominant product upon annealing, which is consistent with calculations that predict no barrier and greater exothermicity for formation of the C_5H_5N−Cl adduct. In contrast, the energies of 2-, 3-, 4-ClC_5H_5N are greater than C_5H_5N−Cl by more than 26 kJ mol^{-1}.[15]

We observed that the intensities of lines of C_5H_5N−Cl attained maxima after irradiation at 365 nm for 1 h and remained nearly constant upon further irradiation. This behavior clearly indicates that the C_5H_5N−Cl radicals either react immediately with *p*-H_2 or Cl atoms or undergo secondary decomposition. This photolytic destruction of C_5H_5N−Cl at 365 nm was confirmed with the difference spectrum recorded after irradiation of an annealed matrix for 12 min, as shown in Fig. 4(c). As we observed production of only C_5H_5N in this experiment, we conclude that C_5H_5N–Cl undergoes secondary photolysis at 365 nm to produce Cl and C_5H_5N. Breslow *et al.* observed an absorption with $\lambda_{max} = 334$ nm that was assigned to C_5H_5N−Cl in solution,[11] supporting that the light of wavelength 365 ± 10 nm employed in this experiment was likely absorbed by C_5H_5N−Cl to induce photolysis.

The photodissociation of gaseous Cl_2 at 365 nm can result in Cl atoms with 38 kJ mol^{-1} of translational energy,[25,26] which is ∼26 kJ mol^{-1} in the center-of-mass coordinates of the Cl + C_5H_5N system. This kinetic energy is greater than the barrier 13 kJ mol^{-1} predicted for formation of 2-C_5H_4N + HCl, but smaller than those, 44 and 37 kJ mol^{-1}, predicted for formation of 3- and 4-C_5H_4N, respectively, with the BB1K/6-31+G(d,p) method.[15] The fact that we observed no major line ascribable to 2-C_5H_4N indicates that either the kinetic energy of Cl was readily quenched before it could find a suitable attacking site to effect H-abstraction or 2-C_5H_4N reacts readily with H_2 to form C_5H_5N. Further isotopic experiments are needed to distinguish these two possible channels.

VI. CONCLUSION

The reaction of Cl atoms with pyridine in solid *p*-H_2 at 3.2 K has been investigated using matrix isolation IR absorption spectroscopy. The most stable planar σ-bonded C_5H_5N–Cl_2 complex was identified in a matrix of $Cl_2/C_5H_5N/p\text{-}H_2$ at 3.2 K; observed shifts in wavenumbers and relative intensities of the IR absorption lines of σ-C_5H_5N-Cl_2 with respect to C_5H_5N isolated in solid *p*-H_2 agree satisfactorily with

the results of quantum-chemical calculations. Upon annealing of the matrix sample $Cl_2/C_5H_5N/p\text{-}H_2$ (3/1/3200) irradiated with UV light at 365 nm, we observed 1-chloropyridinyl ($C_5H_5N{-}Cl$) radical as a major product. The assignments were made according to the expected chemistry, the predicted energy barriers for various reactions, and the anharmonic vibrational wavenumbers and IR intensities predicted with the B3PW91/6-311++G(2d, 2p) method. No other isomeric product such as 2-, 3-, 4-ClC_5H_5N was identified.

ACKNOWLEDGMENTS

National Science Council of Taiwan (Grant No. NSC101-2745-M009-001-ASP) and the Ministry of Education, Taiwan ("Aim for the Top University Plan" of National Chiao Tung University) supported this work. The National Center for High-performance Computing provided computer time.

[1]C. W. Spicer, E. G. Chapman, B. J. Finlayson-Pitts, R. A. Plastridge, J. M. Hubbe, J. D. Fast, and C. M. Berkowitz, Nature (London) **394**, 353 (1998).
[2]H. Boudries and J. W. Bottenheim, Geophys. Res. Lett. **27**, 517, doi:10.1029/1999GL011025 (2000).
[3]O. W. Wingenter, B. C. Sive, N. J. Blake, D. R. Blake, and F. S. Rowland, J. Geophys. Res., [Atmos.] **110**, 20308, doi:10.1029/2005JD005875 (2005).
[4]G. A. Russell, J. Am. Chem. Soc. **79**, 2977 (1957).
[5]C. Walling and M. F. Mayahi, J. Am. Chem. Soc. **81**, 1485 (1959).
[6]P. S. Skell, H. N. Baxter III, and C. K. Taylor, J. Am. Chem. Soc. **105**, 120 (1983).
[7]N. J. Bunce, K. U. Ingold, J. P. Landers, J. Lusztyk, and J. C. Scaiano, J. Am. Chem. Soc. **107**, 5464 (1985).
[8]R. K. Khanna, B. Armstrong, H. Cui, and J. M. Tanko, J. Am. Chem. Soc. **114**, 6003 (1992).
[9]M.-L. Tsao, C. M. Hadad, and M. S. Platz, J. Am. Chem. Soc. **125**, 8390 (2003).
[10]R. Breslow, M. Brandl, J. Hunger, and A. D. Adams, J. Am. Chem. Soc. **109**, 3799 (1987).
[11]R. Breslow, M. Brandl, J. Hunger, N. Turro, K. Cassidy, K. Krogh-Jespersen, and J. D. Westbrook, J. Am. Chem. Soc. **109**, 7204 (1987).
[12]A. Abu-Raqabah and M. C. R. Symons, J. Am. Chem. Soc. **112**, 8614 (1990).
[13]M. L. McKee, A. Nicolaides, and L. Radom, J. Am. Chem. Soc. **118**, 10571 (1996).
[14]J. K. Hao, E. C. Yang, W. D. Wang, X. J. Zhao, and T. H. Tang, J. Mol. Struct.: THEOCHEM **582**, 225 (2002).
[15]S. Parveen and A. K. Chandra, J. Phys. Chem. A **113**, 177 (2009).
[16]Z. Zhao, D. T. Huskey, K. J. Olsen, J. M. Nicovich, M. L. McKee, and P. H. Wine, Phys. Chem. Chem. Phys. **9**, 4383 (2007).
[17]M. J. Almond and A. J. Downs, "Spectroscopy of matrix isolated species," in *Advances in Spectroscopy*, edited by R. J. H. Clark and R. E. Hester (Wiley, Chichester, UK, 1989), Vol. 17, pp. 57–153.
[18]T. Bally, "Matrix isolation," in *Reactive Intermediate Chemistry*, edited by R. A. Moss, M. S. Platz, and M. Jones, Jr. (Wiley, Hoboken, New Jersey, 2004), Chap. 17, pp. 798–840.
[19]P. L. Raston and D. T. Anderson, J. Chem. Phys. **126**, 021106 (2007).
[20]C.-W. Huang, Y.-C. Lee, and Y.-P. Lee, J. Chem. Phys. **132**, 164303 (2010).
[21]B. Golec and Y.-P. Lee, J. Chem. Phys. **135**, 174302 (2011).
[22]J. C. Amicangelo and Y.-P. Lee, J. Phys. Chem. Lett. **1**, 2956 (2010).
[23]J. C. Amicangelo, B. Golec, M. Bahou, and Y.-P. Lee, Phys. Chem. Chem. Phys. **14**, 1014 (2012).
[24]M. Bahou, J.-Y. Wu, K. Tanaka, and Y.-P. Lee, J. Chem. Phys. **137**, 084310 (2012).
[25]P. L. Raston and D. T. Anderson, Phys. Chem. Chem. Phys. **8**, 3124 (2006).
[26]S. C. Kettwich, P. L. Raston, and D. T. Anderson, J. Phys. Chem. A **113**, 7621 (2009).
[27]M. J. Frisch, G. W. Trucks, H. B. Schlegel *et al.*, GAUSSIAN 09, Revision A.02, Gaussian, Inc., Wallingford, CT, USA, 2009.
[28]A. D. Becke, J. Chem. Phys. **98**, 5648 (1993).
[29]J. P. Perdew, K. Burke, and Y. Wang, Phys. Rev. B **54**, 16533 (1996).
[30]A. D. McLean and G. S. Chandler, J. Chem. Phys. **72**, 5639 (1980).
[31]Z. Wang, B. Zheng, X. Yu, X. Li, and P. Yi, J. Chem. Phys. **132**, 164104 (2010).
[32]See supplementary material at http://dx.doi.org/10.1063/1.4789407 for geometries, relative energies, vibrational wavenumbers, and IR intensities of 2-, 3-, 4-C_5H_4N radicals optimized with the B3PW91/6-311++G(2d, 2p) method and spectrum of the C_5H_5N-HCl complex.
[33]J. C. Mackie, M. B. Colket III, and P. F. Nelson, J. Phys. Chem. **94**, 4099 (1990).
[34]J. H. Kiefer, Q. Zhang, R. D. Kern, J. Yao, and B. Jursic, J. Phys. Chem. A **101**, 7061 (1997).
[35]N. R. Hore and D. K. Russell, J. Chem. Soc., Perkin Trans. 2 **1998**, 269.
[36]K. N. Wong and S. D. Colson, J. Mol. Spectrosc. **104**, 129 (1984).
[37]E. Castellucci, G. Sbrana, and F. D. Verderame, J. Chem. Phys. **51**, 3762 (1969).
[38]A. Destexhe, J. Smets, L. Adamowicz, and G. Maes, J. Phys. Chem. **98**, 1506 (1994).
[39]A. J. Barnes, K. Szczepaniak, and W. J. Orville-Thomas, J. Mol. Struct. **59**, 39 (1980).
[40]J. E. D. Bene, W. B. Person, and K. Szczepaniak, Chem. Phys. Lett. **247**, 89 (1995).
[41]K. Szczepaniak, P. Chabrier, W. B. Person, and J. E. D. Bene, J. Mol. Struct. **520**, 1 (2000).
[42]K. Chapman, D. Crittenden, J. Bevitt, M. J. T. Jordan, and J. E. D. Bene, J. Phys. Chem. A **105**, 5442 (2001).
[43]J. M. Kimel'fel'd, A. B. Mostovoy, and L. M. Mostovaja, Chem. Phys. Lett. **33**, 114 (1975).
[44]G. V. Rubenacker and T. L. Brown, Inorg. Chem. **19**, 398 (1980).
[45]L. W. Pickett, M. E. Corming, G. M. Wieder, D. A. Semenow, and J. M. Buckley, J. Am. Chem. Soc. **75**, 1618 (1953).